

Difference in ranges of positrons and electrons in rare-earth metals

R. K. Batra and Bhupender Singh

Physics Department, Punjab Agricultural University, Ludhiana-141004, India

(Received 5 May 1988; revised manuscript received 26 September 1988)

The ranges of positrons and electrons of energies from 0.2 to 5.0 MeV have been computed for all rare-earth metals including scandium and yttrium using the recent range theory based on the combined effects of total-energy loss and the multiple Coulomb scattering. The ratio of the practical range R_p to the continuous slowing-down approximation range R , which indicates the reduction of total path length due to the multiple scattering, varies from 0.25 to 0.80 for positrons and from 0.17 to 0.76 for electrons in lutetium to scandium at 0.2 to 5.0 MeV, respectively. The calculation gives results in better agreement with the known experimental values of the positron range at 1.88 MeV to the electron range at 1.77 MeV in Y, Nd, Ho, and Yb. These calculations also agree well with the semiempirical electron ranges in rare-earth metals.

I. INTRODUCTION

The range of positrons and electrons in different materials is an important penetration parameter for studying theoretically and experimentally the interaction of these particles with matter. The penetration of positrons has been studied¹⁻⁴ using 0.511-MeV annihilation photons and a γ - γ coincidence counting setup. The extrapolated range was extracted from the measured positron-transmitted intensity versus thickness curve. For direct comparison of the penetration of positrons and electrons, many workers¹⁻⁴ also obtained the ranges and mass attenuation coefficients of nearly equal energy electrons in metallic foils by measuring the transmitted intensity of electrons as a function of the absorber thickness using a thin-window Geiger-Muller counter¹ or a gas flow proportional counter.³ The transmission of positrons and electrons was measured under identical geometry. The refined measurements of ranges of positrons in the energy region 0.324–1.88 MeV and those of electrons in the energy region 0.167–3.6 MeV in certain solids and some liquids were reported by Takhar,^{1,4} Patrick and Rupaal,² and Nathu Ram, Sundara Rao, and Mehta.³ Recently it has been resolved³ that the positron penetration is greater than that of equal energy electrons in various solids with the exception of 0.324-MeV particles in Be and Al. To understand the difference in penetration of nearly equal energy positrons and electrons in rare-earth metals, Takhar⁴ extended the measurements of the ranges and mass attenuation coefficients of 1.88-MeV positrons and 1.77-MeV electrons to yttrium, neodymium, holmium, and ytterbium and found an unexpectedly larger penetration of positrons than electrons in rare-earth metals as compared with the neighboring solids studied.

The ratio of experimental positron range to electron range in different elements¹⁻⁴ when compared with Z_d^+/Z_d^- , the ratio of the positron penetration depth to that of the electron calculated on the basis of energy loss and multiple scattering,⁵ reveals that Z_d^+/Z_d^- is not a good index of penetration (for instance, see Fig. 1 of Ref. 4). Recently, Batra and Sehgal⁶ have developed a new method to calculate the practical range (also called the projected range in the literature) of positrons and elec-

trons by considering the total inelastic and the multiple Coulomb elastic scattering with the atomic and nuclear fields of the absorber atoms of different elements. The calculated practical range compares well with the extrapolated range in different materials.⁶

There have been several investigations on the physical properties of rare-earth metals.⁷ The light rare-earth metals (La, Ce–Eu) and the heavy rare-earth metals (Gd–Yb) have shown distinctively different physical properties.⁷ Very few experiments on the penetration of positrons and electrons through rare-earth metals have been carried out and these studies⁴ reflect that positrons and electrons might interact with rare-earth atoms in a different way than the neighboring solids. The theory of penetration of positrons and electrons in rare-earth metals has not been investigated at all. Neither the total path lengths^{6,8} nor the practical ranges of positrons and electrons using range theory⁶ have been computed for each element of the rare-earth series. Moreover, the information about the ranges in rare-earth metals would provide a broader choice of materials in dealing with the problems of radiation shielding. Therefore, we thought it worthwhile to apply the range theory⁶ for calculating the ranges of positrons and electrons in rare-earth metals. This Brief Report contains the details of the calculations of the penetration function $F^+(T)$ and $F^-(T)$, the characteristic random energy T_c^+ and T_c^- and the practical range R_p^+ and R_p^- versus energy T for the rare-earth metals from lanthanum ($Z=57$) to lutetium ($Z=71$) including scandium ($Z=21$) and yttrium ($Z=39$) [scandium ($Z=21$) and yttrium ($Z=39$) whose electronic configurations are similar to the heavy rare-earth metals (Gd–Yb) are also included in the present studies] using the range theory of positrons and electrons in matter.⁶

II. OUTLINE OF THE METHOD

The method of calculation proposed by Batra and Sehgal⁶ depends upon the assumption that positrons and electrons move along the direction of incidence until they lose their energy such that the calculated mean-square projected angle due to multiple scattering on the plane contain-

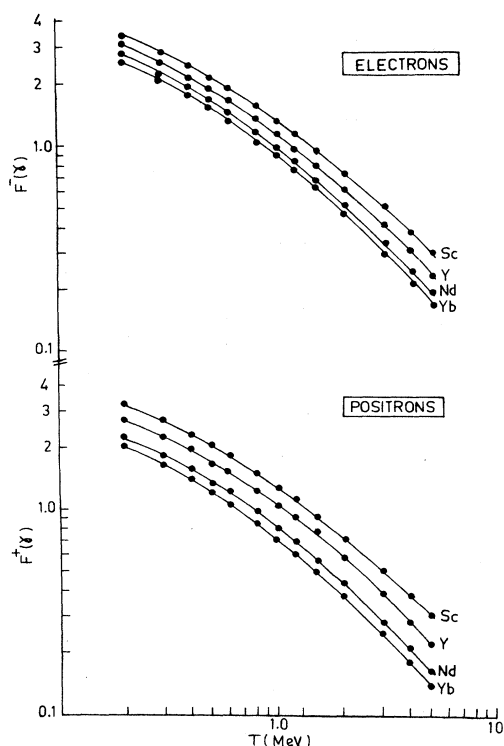


FIG. 1. The filled circles show the calculated $F^+(\gamma)$ and $F^-(\gamma)$ vs kinetic energy of positrons and electrons in Sc, Y, Nd, and Yb. The solid lines are drawn as a visual aid.

ing the initial direction becomes very large. After this stage the particle's motion becomes random, which contributes to straggling only. On the basis of this theory, the mean practical range is given by

$$R_p^\pm(T) = R^\pm(T) - R^\pm(T_c^\pm). \quad (1)$$

The plus and minus superscripts stand for positrons and electrons, respectively. Here, $R^\pm(T)$ and $R^\pm(T_c^\pm)$ are the continuous-slowing-down-approximation (CSDA) ranges at T and T_c^\pm , respectively, and are obtained from

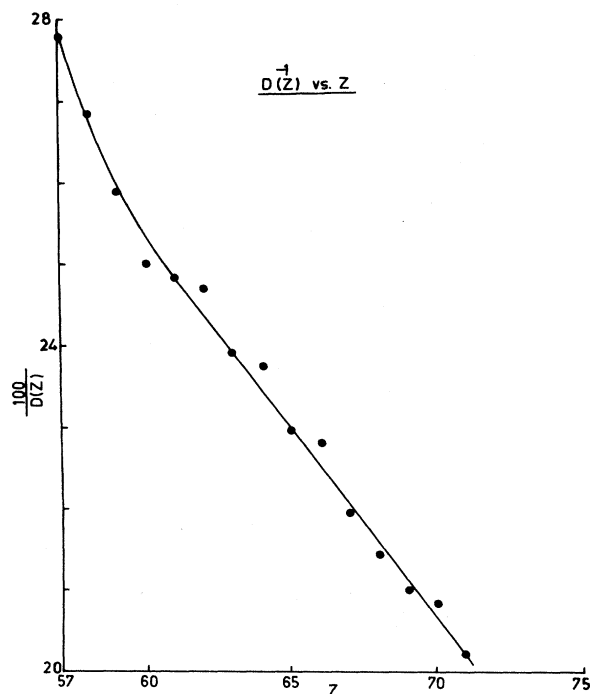


FIG. 2. The function $D^{-1}(Z)$ given by Eq. (3) vs atomic number Z of rare-earth metals (filled circles). The solid line shows the trend.

Eq. (7) of Ref. 8 or from the interpolation of the recently tabulated CSDA ranges by Berger and Seltzer.⁹ The symbols T_c^+ and T_c^- represent, respectively, the characteristic random energy of positrons and electrons of initial energy T relating to the situation when the particles just begin to undergo the random motion. For the estimation of characteristic random energy, the interplay of multiple Coulomb scattering and the total-energy loss of these particles during the penetration are accounted for and, using the definition of transport mean free path, one obtains⁶ a relation

$$F^\pm(\gamma_c) = F^\pm(\gamma) + D^{-1}(Z). \quad (2)$$

TABLE I. Calculated range (mg/cm^2) of positrons (R_p^+) and electrons (R_p^-) in Sc, La, Gd, and Yb at various energies according to Eq. (1).

Energy T (MeV)	Scandium		Lanthanum		Gadolinium		Ytterbium	
	Positron	Electron	Positron	Electron	Positron	Electron	Positron	Electron
0.2	48.7	47.6	28.6	23.6	24.0	18.1	22.2	18.5
0.3	89.5	86.9	47.9	35.0	42.8	36.2	40.4	34.3
0.4	138.0	135.2	74.6	60.0	62.6	62.0	63.9	55.9
0.5	191.0	176.8	109.0	77.5	97.0	84.3	99.7	74.2
0.6	232.1	214.5	145.0	102.0	133.7	113.1	120.1	99.3
0.8	333.4	285.1	227.1	162.4	190.3	166.2	177.3	135.7
1.0	408.3	308.6	264.9	237.3	289.3	216.8	267.3	186.7
1.5	677.9	626.3	440.0	401.9	446.8	365.5	436.5	345.2
2.0	942.8	899.1	741.9	620.9	664.6	545.2	629.2	509.8
3.0	1552.9	1437.4	1159.4	1009.4	1124.4	934.5	1090.5	860.9
4.0	2151.6	2013.9	1646.4	1347.0	1617.1	1306.3	1572.9	1232.2
5.0	2727.7	2545.9	2129.0	1791.5	2085.0	1708.0	2045.7	1630.5

The penetration functions $F^\pm(\gamma)$ are given in Ref. 6, where γ is the total positron or electron energy in units of electron rest mass energy and

$$D^{-1}(Z) = \frac{A(m_2Z + c_2)}{2.044N_0r_0^2Z(Z+1)} \quad (3)$$

where Z , A , N_0 , and $r_0 (=e^2/mc^2)$ are the atomic number, atomic weight of the absorber, Avogadro's number, and the electron radius, respectively. The constants m_2 and c_2 are the same as those occurring in the approximate total-stopping-power-formula⁸ and are listed in Ref. 8.

The values of $F^+(\gamma)$ and $F^-(\gamma)$ at various energies from $T=0.2-5.0$ MeV for all the rare-earth metals have been obtained by solving the integrals⁶ of $F^\pm(\gamma)$ using a computer. Using Eq. (2) and the plot of $F^\pm(\gamma)$ versus energy for rare-earth metal, the value of T_c^+ and T_c^- can be obtained for a given energy. Thus, the practical range R_p^+ of positrons and R_p^- of electrons can be calculated using Eq. (1).

III. RESULTS AND DISCUSSION

Figure 1 shows the behavior of penetration functions $F^+(\gamma)$ and $F^-(\gamma)$ at different energies for scandium, yttrium, neodymium, and ytterbium. The values of $F^-(\gamma)$ are larger than those of $F^+(\gamma)$ for all rare-earth metals at various energies. The difference between $F^-(\gamma)$ and $F^+(\gamma)$ increases slowly with the atomic number of the rare-earth metals for all energies. Figure 2 shows the behavior of the material-dependent function $D^{-1}(Z)$ versus the atomic number Z of the rare-earth metal. It is apparent that the $D^{-1}(Z)$ function decreases nonlinearly for light rare-earth metals, while it decreases linearly for heavy rare-earth metals. The variation of the characteristic random energy T_c^+ and T_c^- versus kinetic energies of positrons and electrons from 0.2–5.0 MeV are shown in

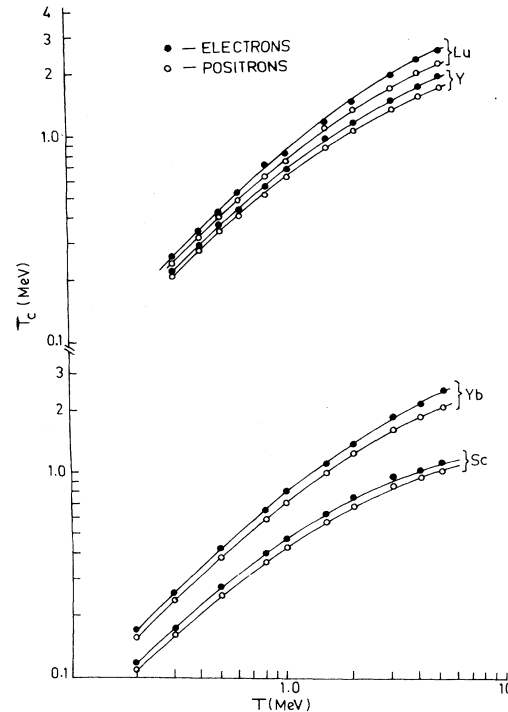


FIG. 3. Calculated values (open and filled circles) of T_c^+ and T_c^- vs kinetic energy of positrons and electrons in Sc, Y, Lu, and Yb. The solid lines are drawn as a visual aid.

Fig. 3. The magnitudes of T_c^+ and T_c^- have significant differences for Sc, Y, Lu, and Yb. The random characteristic energy for electrons is greater than that of positrons for a given T in any rare-earth metal.

Table I contains the practical ranges of positrons and electrons at various energies in Sc, La, Gd, and Yb as computed by the present method. We observe that for a given rare-earth metal, the values of R_p^+ are greater than

TABLE II. Calculated practical range of 1.88-MeV positrons (R_p^+) and 1.77-MeV electrons (R_p^-) in mg/cm^2 for rare-earth metals. The ratio of theoretical range with experimental ratio are also shown.

Element	Atomic number Z	Theoretical		Semiempirical R_{ex}	Theoretical $R_p^+(1.88)/R_p^-(1.77)$	Experimental (Ref. 4)		Theoretical $R_p^+(1.77)/R_p^-(1.77)$
		R_p^+	R_p^-			$R_{ex}^+(1.88)/R_{ex}^-(1.77)$	$R_{ex}^+(1.88)/R_{ex}^-(1.77)$	
Sc	21	879.2	773.6	768.4	1.14(1.16)	1.06
Y	39	737.0	582.5	586.4	1.27(1.24)	1.44	...	1.17
La	57	646.6	447.9	457.7	1.44(1.32)	1.31
Ce	58	646.0	440.4	451.9	1.47(1.33)	1.34
Pr	59	645.4	432.9	447.4	1.49(1.34)	1.38
Nd	60	644.1	431.1	442.6	1.49(1.34)	1.67	...	1.37
Pm	61	634.0	429.3	437.0	1.48(1.35)	1.36
Sm	62	626.6	428.3	432.3	1.46(1.35)	1.34
Eu	63	619.2	427.4	427.3	1.45(1.36)	1.32
Gd	64	611.7	419.1	422.9	1.46(1.36)	1.34
Tb	65	604.3	416.7	417.1	1.45(1.37)	1.34
Dy	66	601.2	413.3	412.4	1.45(1.37)	1.34
Ho	67	598.1	405.7	408.5	1.47(1.37)	1.85	...	1.37
Er	68	590.7	398.2	402.6	1.48(1.38)	1.38
Tm	69	583.2	390.8	397.9	1.49(1.38)	1.40
Yb	70	580.3	383.4	391.7	1.51(1.39)	1.47	...	1.41
Lu	71	577.3	376.0	386.6	1.54(1.40)	1.39

R_p^- at all energies. Further, R_p^+ and R_p^- are larger for a lighter rare-earth element than a heavier rare-earth element. The calculated practical ranges of 1.88-MeV positrons and 1.77-MeV electrons for all rare-earth metals are given in columns 3 and 4 of Table II. Since the measurements of ranges and mass attenuation coefficients of positron and electron in rare-earth metals are sparse, we extract the electron ranges in rare-earth metals semiempirically as follows. Nathu Ram, Sundara, Rao, and Mehta¹⁰ have recently measured the mass attenuation coefficients (μ^-) of electrons at different energies in a larger number of absorbers and formulated an empirical relation whose constants depend upon the atomic number Z of the absorber. They found μ^- for Y, Nd, Ho, and Yb using the interpolated values of the constants for the empirical relation.¹⁰ These values of μ^- are in good agreement with the measurements of μ^- in some rare-earth metals reported by Takhar.⁴ In a recent publication,¹¹ we have given a new method to evaluate μ^- and μ^+ using the range theory⁶ and found that the product of μ^+ or μ^- , the mass attenuation coefficient of positron or electron, and its extrapolated range R_{ex}^\pm for a given absorber is a constant, i.e.,

$$-\mu^\pm R_{ex}^\pm = \ln[I(Z)/I_0], \quad (4)$$

where the values of $I(Z)/I_0$ for Al, Cu, Ag, and Pb are given in Ref. 11. Here we calculate R_{ex}^- using a value of μ^- obtained from the empirical relation¹⁰ and the interpolated value of $I(Z)/I_0$ for a rare-earth metal obtainable from the known¹¹ $I(Z)/I_0$ values for Al, Cu, Ag, and Pb. Column 5 of Table II contains the semiempirical electron range in rare-earth metals obtained using Eq. (4). We find that theoretical values of R_p^- (column 4 of Table II) agree well with the semiempirical R_{ex}^- (column 5 of Table II) for 1.77 MeV electrons in various rare-earth metals.

The ratio of calculated R_p^+ at 1.88 MeV to R_p^- at 1.77 MeV in all rare-earth metals and the ratio of experimental ranges⁴ at these energies in Y, Nd, Ho, and Yb are given, respectively, in columns 6 and 7 of Table II. The values within parentheses in column 6 are the interpolated values of R_p^+/R_p^- for rare-earth metals obtained from the calculated R_p^+/R_p^- in Al, Cu, Ag, Sn, Au, and Pb (see Fig. 9 of Ref. 6). We note that the calculated values are higher by as much as 9% than the interpolated values except in scandium. Thus, the present calculations are in close agreement with the experimental results in Y, Nd, and Yb within the experimental error,⁴ which is stated to be about 7%, while the experimental R_{ex}^+/R_{ex}^- is significantly higher than calculated R_p^+/R_p^- in the case of

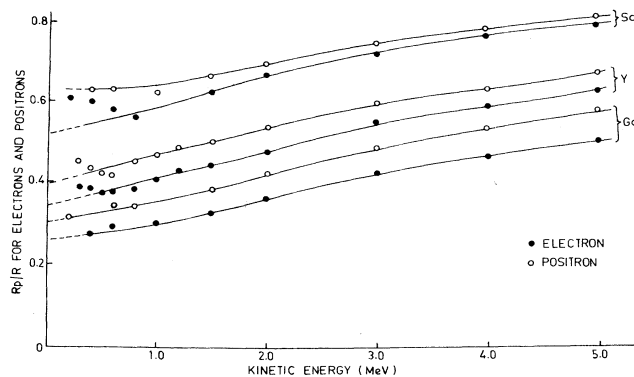


FIG. 4. The ratio of practical range to the CSDA range of positrons (O) and electrons (●) as a function of energy in Sc, Y, and Gd. The solid lines are drawn as a visual aid.

holmium. Further, a part of the larger difference in the penetration of 1.88-MeV positrons and 1.77-MeV electrons is attributable to the 6% difference in the initial energies of the particles. The idea of this difference can be obtained by studying the theoretical ratios of $R_p^+(1.88)/R_p^-(1.77)$ and $R_p^+(1.77)/R_p^-(1.77)$ given in column 6 and column 8, respectively, of Table II for all rare-earth metals. Therefore, the future measurements of the ranges of equal energy positrons and electrons in rare-earth metals would throw light on the actual difference in the interactions of positrons and electrons with the atoms of rare-earth metals.

Finally, the variations of R_p^+/R^+ and R_p^-/R^- versus energy in Sc, Y, and Gd are depicted in Fig. 4. This ratio is greater for positrons than electrons in a rare-earth metal at any energy and it decreases more rapidly for a heavier rare-earth metal than a lighter one. The reduction in the CSDA range due to the inclusion of multiple scattering lies between 0.25 and 0.80 for positrons and between 0.17 to 0.76 for electrons in lutetium and scandium, respectively, at the extreme energies considered. Thus, we conclude that the interplay of inelastic and multiple Coulomb scatterings is such that the practical range of positrons is always longer than that of the equal-energy electrons in all the rare-earth metals. Further, these calculations clearly show that the rare-earth metals constitute a distinctive group in the Periodic Table with the relatively larger difference in penetration of positrons and electrons than the neighboring solids. This behavior might be associated with some property of the rare-earth atoms or nuclei and needs to be explored theoretically as well as experimentally.

¹P. S. Takhar, Phys. Rev. **157**, 257 (1967).

²J. R. Patrick and A. S. Rupaal, Phys. Lett. A **35**, 235 (1971).

³Nathu Ram, I. S. Sundara Rao, and M. K. Mehta, Phys. Rev. A **23**, 1202 (1981).

⁴P. S. Takhar, Phys. Lett. **28A**, 423 (1968); and in *Proceedings of the Fourteenth Rare-Earth Research Conference, Fargo, North Dakota, 1979*, edited by G. J. McCarthy, J. J. Rhyne, and H. B. Silber (Plenum, New York, 1980), Vol. 2, p. 287.

⁵F. Rohrllich and B. C. Carlson, Phys. Rev. **93**, 38 (1954).

⁶R. K. Batra and M. L. Sehgal, Phys. Rev. B **23**, 4448 (1981).

⁷K. A. Gschneidner, Jr. and Le Roy Eyring, *Handbook on*

Physics and Chemistry of Rare Earths (North-Holland, Amsterdam, 1978), Vol. 1, p. 233.

⁸R. K. Batra and M. L. Sehgal, Nucl. Instrum. Methods **109**, 565 (1973).

⁹M. J. Berger and S. M. Seltzer, *Stopping Powers and Ranges of e^- and e^+* , 2nd ed., Natl. Bur. Stand. (U.S.) Tech. Rep. No. 82-2550-A (U.S. GPO, Washington, DC, 1982).

¹⁰Nathu Ram, I. S. Sundara Rao, and M. K. Mehta, Pramana **18**, 121 (1982).

¹¹Bhupender Singh and R. K. Batra, Int. J. Appl. Radiat. Isot. **38**, 1027 (1987).